Phasematching in semiconductor nonlinear optics by linear long-period gratings

Cite as: Appl. Phys. Lett. **92**, 181110 (2008); https://doi.org/10.1063/1.2918013
Submitted: 08 February 2008 • Accepted: 09 April 2008 • Published Online: 09 May 2008

Alex Hayat, Yotam Elor, Eran Small, et al.

Phasematching in semiconductor nonlinear optics by linear long-period gratings

Alex Hayat,[1,a)] Yotam Elor,[2] Eran Small,[3] and Meir Orenstein[1]
[1]*Department of Electrical Engineering, Technion, Haifa 32000, Israel*
[2]*Department of Computer Science, Technion, Haifa 32000, Israel*
[3]*Physics Department, Weizmann Institute of Science, Rehovot 76100, Israel*

(Received 8 February 2008; accepted 9 April 2008; published online 9 May 2008)

We experimentally demonstrate a phasematching technique for frequency conversion in nonlinear semiconductor structures by employing linear long-period gratings. We designed a specific semiconductor photonic device for second harmonic generation using coupled-mode equations with parameters extracted from beam propagation method simulations. Optical frequency converters were fabricated according to the design with the main feature; linear long-period weak gratings imprinted on semiconductor waveguides, providing the required photon momentum difference for matching the phases of the different-wavelength photons. The measured nonlinear conversion efficiency and its spectrum comply with our theoretical predictions. © *2008 American Institute of Physics*. [DOI: 10.1063/1.2918013]

Phasematching is crucial for achieving high efficiency optical frequency conversion. Two prominent techniques for phasematching realization are the dispersion management by material anisotropy or by structure,[1–4] to match the phase velocities of the various photons involved in the process, and quasi-phase-matching[5] (QPM), mostly in periodically poled ferroelectric crystals, where the second-order nonlinear susceptibility $\chi^{(2)}$ is spatially modulated with the appropriate period, shorter than the conversion coherence length.

Here, we design and realize a device based on a different route for phasematching, namely, the use of spatial modulation of only the linear refractive index of the waveguide. The resulting long period grating structure is similar to that used to couple between two modes or waveguides in photonic circuitry (grating-assisted couplers[6]), however, rather than matching the propagation constants of two different modes at a single frequency, here the grating modifies the photon momentum for each wavelength involved in the interaction. Linear long-period gratings, which were theoretically proposed for phasematching using spatial harmonic matching in bulk materials,[7,8] have not been experimentally realized yet. Furthermore, the fact that in bulk materials it is difficult to separate the nonlinear and linear spatial modulation effects has prevented the realization of such techniques so far. Short-period gratings and photonic crystals have been employed to modify the dispersion for efficient nonlinear processes[9] and for microcavity realization,[10] however, they require very high resolution and accuracy of both design and fabrication.

Semiconductors nonlinear frequency converters may be highly useful due to their very high second-order nonlinear susceptibilities accompanied by very mature processing technology, which allows the realization of compact waveguides—an indispensable advantage for achieving high field intensities with long interaction lengths. However, optical isotropy of semiconductors prevents natural birefringent phasematching, while the existing QPM techniques in semiconductors[11–14] require complex epitaxial growth or wafer bonding. A promising technique was recently introduced based on combining artificial birefringence with tight confinement,[15] however, it requires very specific materials for the selective oxidation based fabrication. Semiconductor quantum structures such as quantum wells (QWs) can be designed to meet particular requirements of specific optical response and frequency range,[16,17] which is a distinct advantage over bulk materials with a predetermined response spectrum. It is appealing to apply long-period linear grating phasematching to semiconductor waveguides with embedded QWs as a nonlinear medium, benefiting from the easy fabrication of such structures and the ability to spatially modulate the linear index of refraction without modulating the nonlinearity.

We designed a nonlinear wavelength converter based on GaInP QW structure embedded in a AlGaInP ridge waveguide. Waveguide transverse modal field distributions for the pump $\xi_\omega(x,y)$ (having near 1.48 μm central wavelength) and the second harmonic (SH) fields $\xi_{2\omega}(x,y)$ were calculated using mode-solving based on finite-difference beam propagation method[18] (BPM), which employs propagation along an imaginary distance as a means for sorting modes, under a general excitation (Fig. 1). A spatial periodic perturbation $\Delta\chi^{(1)}(z)$, providing the photon momentum difference required for phasematching, is added by small periodical changes in the ridge waveguide height. Since the modulation is performed only at the tails of the optical field distributions, where the overlap with the nonlinear medium is negligible, mostly the linear coefficient of the waveguide is modulated, whereas the highly nonlinear QW layer[19] remains unperturbed.

For the design, we solved the coupled-mode equations for the amplitudes of the pump and SH slowly varying envelopes, $A_\omega(z)$ and $A_{2\omega}(z)$, respectively, applying conventional initial conditions and nondepleted pump approximation.[20] The resulting amplitudes are

$$A_\omega(z) = A_0 \exp\left\{-iC_1 \int_0^z \Delta\chi^{(1)}_{(z')} dz'\right\} \tag{1}$$

for the pump field and

a)Electronic mail: ahayat@tx.technion.ac.il.

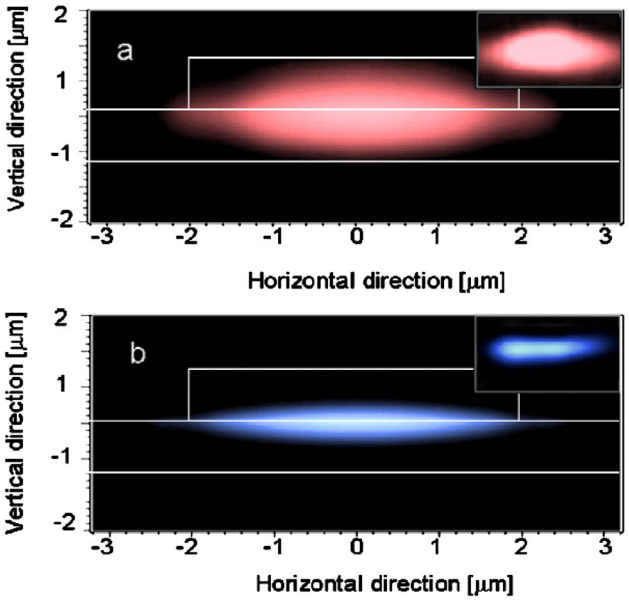

FIG. 1. (Color online) (a) Calculated fundamental mode at the pump wavelength 1480 nm. White lines outline the waveguide's structure. (b) Calculated fundamental mode at the SHG wavelength 740 nm. The insets are the measured modes.

$$A_{2\omega}(z) = iC_3A_0^2 \exp\left\{-i\int_0^z \Delta\chi^{(1)}_{(z')}C_2dz'\right\}\cdot\int_0^z \exp\left\{-i\left[\Delta\beta z' + \int_0^{z'}(C_2-2C_1)\Delta\chi^{(1)}(z'')dz''\right]\right\}dz \tag{2}$$

for the SH field. $\Delta\beta=2\beta_\omega-\beta_{2\omega}$ is the propagation constant difference, while the linear perturbation coefficients C_1, C_2, and the nonlinear coupling coefficient C_3 are given by

$$C_1 = \frac{\omega\varepsilon_0}{4}\int_{-\infty}^{\infty}\int_{-\infty}^{\infty}\xi_\omega^2(x,y)\Delta\chi_\omega^{(1)}(x,y)dxdy,$$

$$C_2 = \frac{\omega\varepsilon_0}{2}\int_{-\infty}^{\infty}\int_{-\infty}^{\infty}\xi_{2\omega}^2(x,y)\Delta\chi_{2\omega}^{(1)}(x,y)dxdy,$$

$$C_3 = \frac{\omega}{2}\int_{-\infty}^{\infty}\int_{-\infty}^{\infty}\xi_{2\omega}(x,y)\xi_\omega^2(x,y)d_{eff}(x,y)dxdy, \tag{3}$$

with $d_{\text{eff}}=\chi^{(2)}/2$. It is important to note that here the linear spatial modulation causes only self-coupling, i.e., modification of the propagation constant of the mode itself, in contrast to cross-coupling which is used in grating assisted couplers between modes or in QPM between different wavelengths.

For harmonic perturbation $(C_2-2C_1)\Delta\chi(z)=D_0\cos(2\pi/\Lambda z)$, the SH amplitude is

$$|A_{2\omega}(L)| = |C_3A_0^2|\cdot\left|\int_0^L \exp\left\{-i\left[\Delta\beta z' + \frac{D_0}{k_g}\sin(k_gz')\right]\right\}dz'\right|, \tag{4}$$

where $k_g=2\pi/\Lambda$ with Λ as the linear grating period.

In the limit of a large number of grating periods, only the integer values of $\Delta\beta/k_g$ yield a nonvanishing SH output. The grating period Λ was chosen to achieve $\Delta\beta/k_g=1$ in order to reach the maximal efficiency, whereas choosing $\Delta\beta/k_g$ to be an integer greater than 1 would reduce the efficiency

$$|A_{2\omega}(L)| = \left|C_3A_0^2L\cdot J_{\Delta\beta/k_g}\left(\frac{D_0}{k_g}\right)\sin c\left[\frac{L}{2}(k_g-\Delta\beta)\right]\right|, \tag{5}$$

where J_i designates a Bessel function of order i.

The overall process efficiency for the first-order optimal case where $k_g=\Delta\beta$ is

$$\frac{P_{2\omega}}{P_\omega^2} = \frac{2C_3^2L^2J_1(D_0/\Delta\beta)^2\beta_{2\omega}^2n_{2\omega}}{\sqrt{\varepsilon_0\mu_0}\cdot\omega\beta_{2\omega}n_\omega^2} \tag{6}$$

with n_ω and $n_{2\omega}$ as effective indices at the pump and the SH wavelengths, respectively.

Using this model, we have designed and fabricated photonic devices for SH generation (SHG) with linear long period gratings for phasematching using samples consisting of four periods of compressively strained 50 Å $Ga_{0.45}In_{0.55}P$ QWs separated by 55 Å $(Al_{0.5}Ga_{0.5})_{0.51}In_{0.49}P$ barriers, ~1.1 μm AlGaInP lower cladding and ~0.5 μm AlGaInP upper cladding. The lateral light confinement was achieved by a 4 μm wide ridge waveguide, realized by etching techniques. The propagation constants of the fundamental pump and SH modes were calculated to be $\beta_1=12.8\ \mu\text{m}^{-1}$ and $\beta_2=28\ \mu\text{m}^{-1}$. Considering both the material and the modal dispersion, the grating period was designed to be $\Lambda=2.7\ \mu$m with 100 nm depth.

For a 50-period linear grating, the wavelength dependence of the conversion efficiency was calculated [using Eq. (5)] to be centered at 1480 nm with ~26 nm bandwidth. The actual integrated devices were fabricated by focused ion beam (FIB) milling (FEI Strata 400) system (Fig. 2). The milling system was operated at an acceleration voltage of 30 kV with a beam dwell time of 1 μs, a 40% overlap, and a current of 1.6 nA, corresponding to a beam diameter of 0.5 μm. Subsequently, the waveguide device was cleaved to the length of ~1 mm, however, only 50 periods (~135 μm overall length) of the weak (100 nm deep) perturbation were milled due to the limited FIB one-take milling area for a given resolution. Such long-period grating structures can be

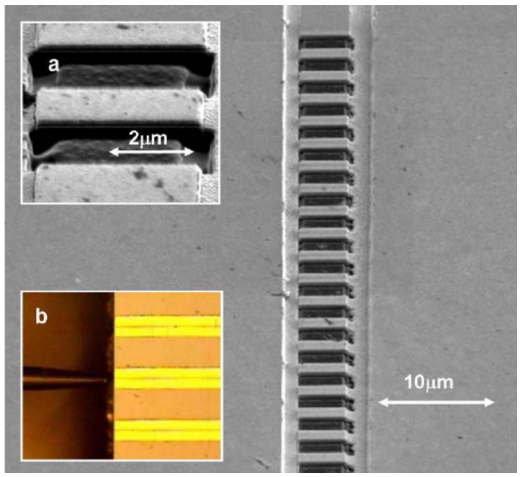

FIG. 2. (Color online) Scanning electron microscopy (SEM) image of the fabricated device. The insets are (a) magnified SEM image of the device and (b) a optical microscope image of the fiber coupling to the waveguide.

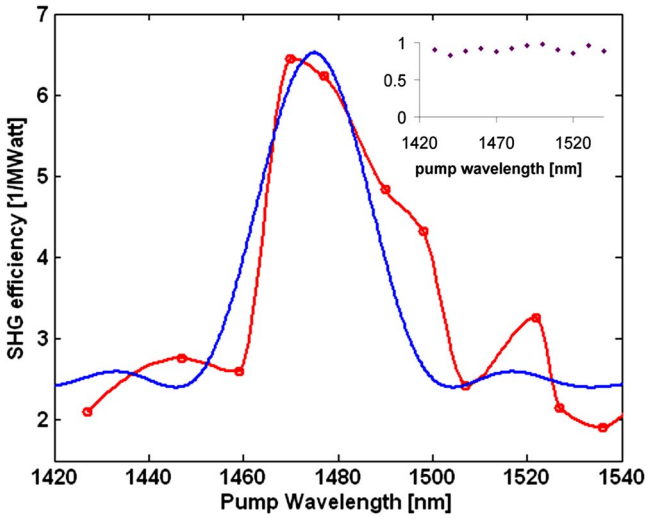

FIG. 3. (Color online) SHG efficiency P_{SH}/P_{pump}^2 vs pump wavelength. The theoretical prediction for 50 grating cycles—blue line, and the experimental results—red line with circles indicating the actual measured points. The inset shows normalized SH efficiency measurements with a similar waveguide without the perturbation.

fabricated in principle by the more conventional photolithography; however, FIB milling allows faster maskless design-fabrication cycles.

The resulting nonlinear waveguide converter was tested by injecting an optical pump using ~130 fs pulses from an optical parametric oscillator (OPO) at telecommunication wavelengths (1420–1550 nm) with a 80.8 MHz repetition rate and an average power of ~100 mW. The OPO was pumped by a mode-locked Ti:sapphire laser at 810 nm. To avoid two-photon based luminescence, special care was taken to pump the structure at wavelengths significantly above the resonant two-photon absorption edge of $Ga_{0.45}In_{0.55}P$ (at ~1340 nm). The pump pulses were facet coupled into the waveguide with about 2 μm^2 mode area by a polarization maintaining lensed fiber [Fig. 2 inset (b)], after filtering out the residual Ti:sapphire 810 nm pump by a thick GaAs layer. The generated SH light was fiber-coupled from the output facet into an ANDO spectrum analyzer with optical output, serving as a tunable 10 nm band-pass filter, and the photons were detected at room temperature by a photon counting module (Perkin-Elmer—SPCM 14) with ~70% efficiency at the SH wavelengths (710–775 nm).

The measured wavelength dependence of the SHG efficiency, P_{out}/P_{in}^2, matches well the calculated one (Fig. 3), in contrast to a nearly flat conversion efficiency spectrum measured in a similar waveguide with no grating (Fig. 3), while the quantitative effect of the phasematching can be estimated by comparing the phasematched peak response to the nonphasematched background (Fig. 3). The spectrum was measured with 10 nm resolution—similar to the actual pump's nominal spectral width. Far from the optimal phasematched wavelength (~1480 nm) the main contribution to SHG efficiency is rather from the nonphasematched bulk nonlinearity which was not considered in the design and thus is equally mismatched for the entire spectrum presented. The overall efficiency of the specific realized converter per unit length squared is ~6% $W^{-1}\,cm^{-2}$ (Fig. 3). The absolute-efficiency precision in this experiment is mostly determined by the coupling variations. The SH power was normalized to the measured out-coupled pump power and therefore the uncertainty in the setup is due to the ±3 dB variations of the coupling to the detector. Thus, the overall efficiency of the current experiment is $3\%-12\%/W/cm^2$. The relative precision of the experimental points in Fig. 3 is ~1% and is mostly determined by the photon counter integration times (about 1 min), while for a given waveguide the losses were constant.

The linear loss due to the grating cannot be directly measured by this setup due to the dominance of the overall coupling loss variations from waveguide to waveguide (~9 bB). The relatively weak perturbation (100 nm depth) is expected to yield only small loss—calculated by BPM to be ~0.23 dB for the 135 μm grating (<17 dB/cm). This value is of the same order as the best reported results for QPM (Ref. 12) (6 dB/cm) and artificial birefringence[15] (23 dB/cm).

The conversion efficiency is similar to those of the reported semiconductor modal phasematching[15] efficiencies, and two orders of magnitude lower than that of semiconductor QPM schemes[12,21]. The difference mainly stems from the small modal confinement factor, namely the small overlap of the optical modes with the four 5 nm thick QWs (about a few percent). Increasing the number of QWs to ~40 should result in efficiencies as high as 600% $W^{-1}\,cm^{-2}$—close to the best results reported using alternative phasematching in semiconductors, while optimization of the grating period and envelope shapes may further enhance the efficiency.

In conclusion, we have experimentally demonstrated a method of long-period linear grating phasematching for highly nonlinear semiconductor structures. The measured frequency response of the designed and fabricated devices nonlinear efficiency is in good agreement with our theoretical result.

[1] G. Klemens, C.-H. Chen, and Y. Fainman, Opt. Express **13**, 9388 (2005).
[2] Z. Yang, P. Chak, A. D. Bristow, H. M. van Driel, R. Iyer, J. S. Aitchison, A. L. Smirl, and J. E. Sipe, Opt. Lett. **32**, 826 (2007).
[3] G. Leo and E. Rosencher, Opt. Lett. **23**, 1823 (1998).
[4] D. Pezzetta, C. Sibilia, M. Bertolotti, J. W. Haus, M. Scalora, M. J. Bloemer, and C. M. Bowden, J. Opt. Soc. Am. B **18**, 1326 (2001).
[5] K. Banaszek, A. B. U'Ren, and I. A. Walmsley, Opt. Lett. **26**, 1367 (2001).
[6] A. Yariv, *Introduction to Optical Electronics* (Holt, New York, 1971).
[7] S. Somekh and A. Yariv, Appl. Phys. Lett. **21**, 140 (1972).
[8] T. Suhara and H. Nishihara, IEEE J. Quantum Electron. **26**, 1265 (1990).
[9] J. W. Haus, R. Viswanathan, M. Scalora, A. G. Kalocsai, J. D. Cole, and J. Theimer, Phys. Rev. A **57**, 2120 (1998).
[10] A. Hayat and M. Orenstein, Opt. Lett. **32**, 2864 (2007).
[11] S. Ducci, G. Leo, V. Berger, A. De Rossi, and G. Assanto, J. Opt. Soc. Am. B **22**, 2331 (2005).
[12] X. Yu, L. Scaccabarozzi, J. S. Harris, Jr., P. S. Kuo, and M. M. Fejer, Opt. Express **13**, 10742 (2005).
[13] K. L. Vodopyanov, O. Levi, P. S. Kuo, T. J. Pinguet, J. S. Harris, M. M. Fejer, B. Gerard, L. Becouarn, and E. Lallier, Opt. Lett. **29**, 1912 (2004).
[14] O. Levi, T. J. Pinguet, T. Skauli, L. A. Eyres, K. R. Parameswaran, J. S. Harris, Jr., M. M. Fejer, T. J. Kulp, S. E. Bisson, B. Gerard, E. Lallier, and L. Becouarn, Opt. Lett. **27**, 2091 (2002).
[15] L. Scaccabarozzi, M. M. Fejer, Y. Huo, S. Fan, X. Yu, and J. S. Harris, Opt. Lett. **31**, 3626 (2006).
[16] J. Khurgin, Phys. Rev. B **38**, 4056 (1988).
[17] P. Ginzburg, A. Hayat, and M. Orenstein, J. Opt. A, Pure Appl. Opt. **9**, S350 (2007).
[18] S. Jungling and J. C. Chen, IEEE J. Quantum Electron. **30**, 2098 (1994).
[19] A. Fiore, E. Rosencher, V. Berger, and J. Nagle, Appl. Phys. Lett. **67**, 3765 (1995).
[20] R. W. Boyd, *Nonlinear Optics* (Academic, New York, 1992).
[21] S. Venugopal Rao, K. Moutzouris, and M. Ebrahimzadeh, J. Opt. A, Pure Appl. Opt. **6**, 569 (2004).